

# Aerodynamic Study of the Ahmed Body in Road-Situations using Computational Fluid Dynamics

R. Manimaran

Thermal and Automotive Research Group  
School of Mechanical and Building Sciences  
VIT University (Chennai campus)

Vandalur – Kelambakkam road, Chennai, Tamilnadu 600127  
India  
manimaran.nr@gmail.com

*Abstract:-* The vehicle aerodynamics is of day to day interest in upcoming new concept vehicles owing to the fuel savings. The present work aims to discover the flow pattern of Ahmed body on the road during the acceleration and overtaking the vehicle to the right. The aerodynamic characteristics such as lift and drag coefficients are compared. Computational Fluid Dynamics (CFD) simulations predict the on-road condition after validation with the experimental results in the wind tunnel. OpenFOAM software is used for CFD analyses. Further drag reduction is achieved by constructing the platoon of two vehicles separated by 0.2 and 0.3 vehicle lengths and the associated interference drag with the isolated case are compared.

*Key-words:-* Ahmed body, Flow field, Drag coefficient, Overtaking, Platooning, Computational fluid dynamics.

## 1. Introduction

Aerodynamic drag of a typical passenger car arises from the styled upper surfaces and the underbody and wheels. The major drag component comes from the upper surfaces, especially in the separated flow regions at the rear base of the car. While a significant amount of research has been conducted on the effect of base cavities on drag reduction for axi-symmetric bodies at high Mach numbers relevant to missile aerodynamics, very few studies have been at the low subsonic Mach numbers relevant for automobiles.

In contrast, road driving is in the influence of turbulent atmospheric winds and traffic wakes. These factors influence the relative wind environment experienced by the moving vehicle to one which has significant temporal and spatial variations. Recently, road vehicle aerodynamic research has increasingly been focussed on understanding the flow field in the environment. Much data are obtained from the wind engineering simulation of a correctly scaled model in the wind tunnel.

Abdel Azim and Abdel Gawad (2000) carried out a flow visualization study of the aerodynamic interference between passenger cars in different moving arrangements. Abdel Azim and Abdel Gawad (2000) performed a numerical investigation of the aerodynamics of a bus and a

van through driving tunnels. Himeno et al. (1990) analyzed numerically the airflow around vehicles using multi-block structured grids. Kitoh et al. (1986) used K- $\epsilon$  model to study the effect of boundary layer conditions on flow around a two-dimensional vehicle. Ahmed and Hucho (1977) used the panel method to calculate the flow past a van. Minato et al. (1991) carried out an experimental research to clarify the wake structure behind trucks. Results of flow visualization and image processing were compared with the finite volume results using K- $\epsilon$  model. They stated that the drag coefficient in overtaking process depends on the relative position of the two vehicles during the process.

Smoke flow visualisations show a clear difference in the wake pattern for various inter-vehicle gaps, as the gap is varied. In the platooning of 0.2 and 0.3 vehicle length spacings, the drag coefficient is observed to be less. The value of drag coefficient agrees with typical values from the literature (Ahmed et al., 1984). The present aim of the work is to study the flow field around the Ahmed body during acceleration conditions and overtaking the vehicle at the right side. Further the stream lines and pressure contours of the flow field are investigated. The turbulent kinetic energy is compared between different cases and computed. The literature survey gives a variety of computational to experimental studies. In this present study, consideration is emphasized on CFD for overtaking and platooning like in roads.

## 2. Methodology

CFD tool is presently used nowadays to explore the flow phenomena as depicted in real life situations. The modeling of the Ahmed body (Fig. 1) is performed in Salome software. The model is meshed using the SnappyHexMesh tool under OpenFOAM.

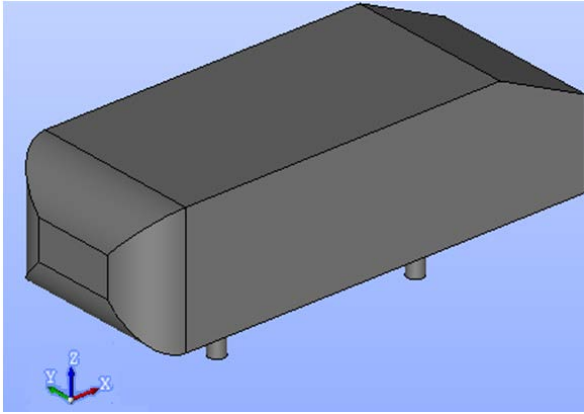


Figure 1. Model of the Ahmed body

The mesh population is varied from from 0.1 million to 1.5 million. From the Figure 2., it is found that average coefficient of drag does not vary after 0.8 million. The cell count near to 0.8 million is considered during all the simulations. The OpenFOAM results are in close conformity with the software. PISO solver is implemented to represent the steady and incompressible flow situation in this problem. Large eddy simulation model is considered in the simulation. Paraview software is used for post-processing the steady state results of pressure contour and velocity streamlines. Grid independency test (Fig. 2) is carried out and matched with the experimental results of Ahmed et al (1984). The inlet condition is specified as the velocity inlet, while the outlet as pressure outlet. No slip conditions are specified on the surfaces of the Ahmed body and walls. The meshing of the Ahmed body is presented in Figure 3.

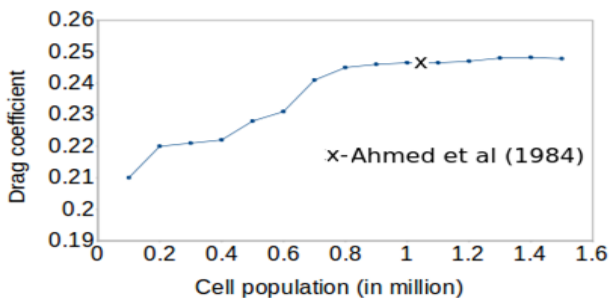


Figure 2. Grid independency test

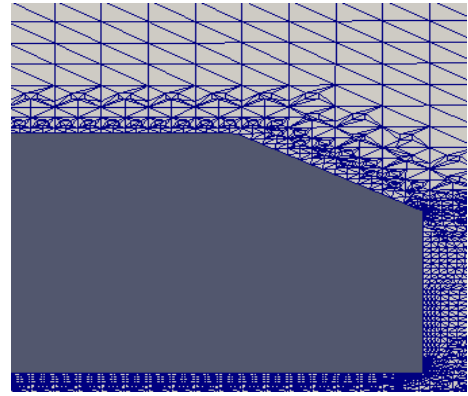


Figure 3. Mesh (0.8 million) shown in rear end of Ahmed body

The analyses were performed in steady state, adiabatic, fully turbulent conditions, for a reference pressure and temperature of the air  $p_{\infty} = 1$  bar and  $T_{\infty} = 15$  °C. These were used for computation of the rest of the air free stream parameters, as density and viscosity. The reference velocity of free stream was  $v_{\infty} = 40$  m/s ( $Re = 2.63 \times 10^6$ , Reynolds number computed with the Ahmed body length, 1) and the turbulence intensity was set to 0.2 %.

To model the turbulent flow around the Ahmed body, large eddy simulation model is used. The main idea behind LES is to reduce this computational cost by reducing the range of time- and length-scales that are being solved for via a low-pass filtering of the Navier–Stokes equations. Such a low-pass filtering, which can be viewed as a time- and spatial-averaging, effectively removes small-scale information from the numerical solution. This information is not irrelevant and needs further modeling, a task which is an active area of research for problems in which small-scales can play an important role such as near-wall flows. Large turbulent structures in the flow are resolved by the governing equations, while the effect of the sub-grid scales (SGS) are modelled using LES-Smagorinsky model [8]. The scale separation is obtained by applying a filter to the governing equations which also influences the form of the SGS models.

## 3. Results and Discussion

### 3.1 Validation

Following the grid independency study, studies are conducted to validate the geometry and compare with the published results in literature. The results of the simulation are validated with

the experimental data from the literature [9] for the base case i.e. when the Ahmed model is not accelerated and not overtaken. From the Figure 4, it can be found that five stations are considered at the rear end of the Ahmed body. The velocity and turbulent kinetic energy are compared between the present work using LES model and the experimental work by Emmanuel [9]. Figure 4 shows the results obtained in the OpenFOAM code at the rear end of the Ahmed body as illustrated in the same figure. Five stations a-e are identified and the velocity magnitude and turbulent kinetic energy data are obtained and found to be within 5 % of the experimental data from Emmanuel [9]. The freestream velocity value converges to 50 m/s as flow is out from the boundary layer.

### 3.2 Acceleration of Ahmed model

The Ahmed model is simulated at wind speeds of 20, 30 and 40 m/s and the lift and drag values are monitored and tabulated in Table 1. It is found that the drag and lift coefficients increase with wind speed. The converged results are obtained after 419 iterations. The pressure contours are shown in Fig. 5 for the speed 20 m/s, 30 m/s and 40 m/s. It can be easily verified that the pressure increases in the fore front of the Ahmed body while the pressure decreases to a much wider region around the Ahmed body in the upper and rear parts of the Ahmed body. The pressure arises due to the presence of bluff body feature while facing the flow (compression) and decreases due to sharp turning of the flow causing the expansion at the rear end of the body.

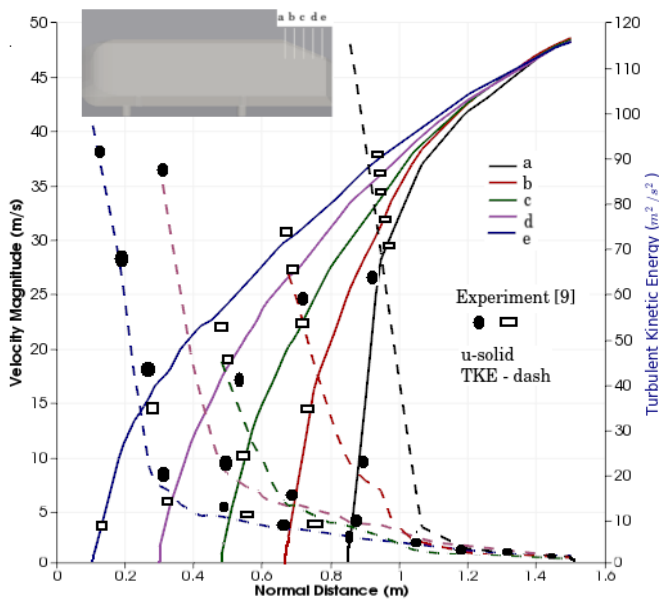


Figure 4. Validation of present model with experimental data [9]

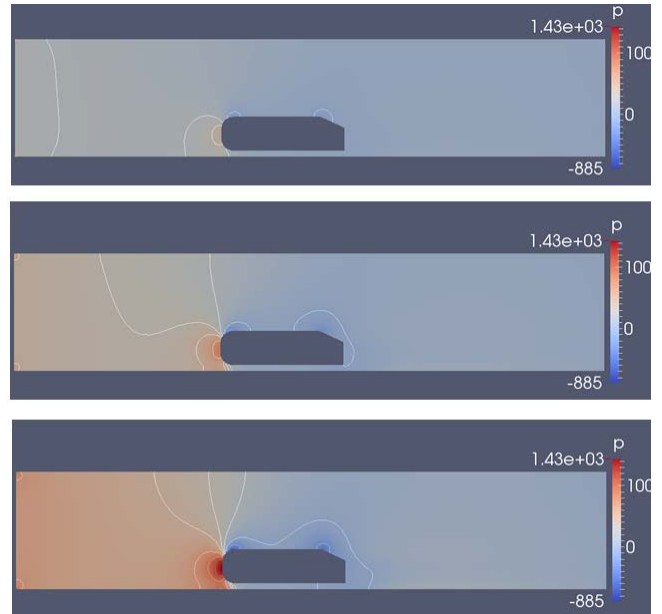


Figure 5. Pressure contours during acceleration, top to bottom : 20 m/s, 30 m/s and 40 m/s

Table 1.  $C_D$  and  $C_L$  for the acceleration of the Ahmed body

Speed (m/s)	Coefficient of Drag, $C_D$	Coefficient of Lift, $C_L$
20	0.284	0.514
30	0.286	0.528
40	0.287	0.536

The flow field is better visualized with the help of streamlines and shown in Figure 6. The vortex structure behind the wake of Ahmed body is noticed from the Fig. 6. Vortices are formed behind the end of Ahmed body. The stream lines show an increase in the vortex motion as the wind speed progresses with the greatest unsteadiness occurring around the periphery of the trailing vortices. This is expected from the difference in the pressures near the rear-pillar, results in the rear-pillar trailing vortices. The comparisons encourage the investigation of the flow details by utilizing the CFD simulation results. the two strong counter-rotating vortices emanating from the slant are present and the flow separates in the middle region of the top edge and reattaches on the slant. The attached flow on the diffuser generate an under-pressure that forms longitudinal vortices on each side of the body. They counter-rotate to the longitudinal vortices coming from the rear end i.e. the upper part of the vehicle. They are created

from the low pressure generated by the diffuser at the rear underhood of the Ahmed body. Further downstream the upper vortices will dominate and their core of rotation was located close to ground. This would eventually decay and transfer into longitudinal components leading to turbulence.

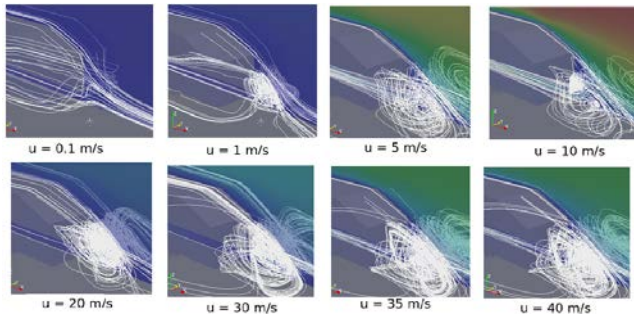


Figure 6. Velocity streamlines during the acceleration

### 3.3 Overtaking

The overtaking vehicle is at the right (at 40 m/s) and the vehicle to be overtaken (at 30 m/s) is at the left as shown in pressure contour (Fig. 7a and Fig. 7b). The flow generated by the movement of a another vehicle is found to influence on drag and lift as shown in Table 2. The drag coefficient decreases for the vehicle to be overtaken and increases for the vehicle that overtakes. The reason could be clearly explained with the help of Fig. 7 as the pressure contours show increase in upstream pressure in the case when the vehicle is overtaken. The pressure build up upstream and net pressure change between the upstream and downstream contributes to high drag. The lift is generated mainly by the pressure difference between the under and upper surfaces of the car. So it is benefit to improve the understanding of the influence of the combined flow on lift by examining the distribution of static pressure on the model surface. The results show that the vortices which originate at the rear of the vehicle have a major impact on the bluff body aerodynamics. By checking the horse shoe vortices in wake region, it is noticed that, at lower speeds, the upper vortex is the dominant vortex; with the increase of speed, the lower vortex is intensified, and becomes the dominant vortex at higher speeds. When the upper and lower vortices achieve a relative equilibrium, the drag reaches the minimum value. The momentum increase intensifies the lower vortex, and results in the relative equilibrium of upper and lower vortices being achieved at a lower speed.

Table 2. Aerodynamic coefficients during the overtaking case

Overtaking vehicle		Vehicle to be overtaken	
$C_D$	$C_L$	$C_D$	$C_L$
0.282 (behind)	0.521	0.283	0.521
0.294 (side)	0.531	0.276	0.507
0.299 (front)	0.542	0.279	0.494

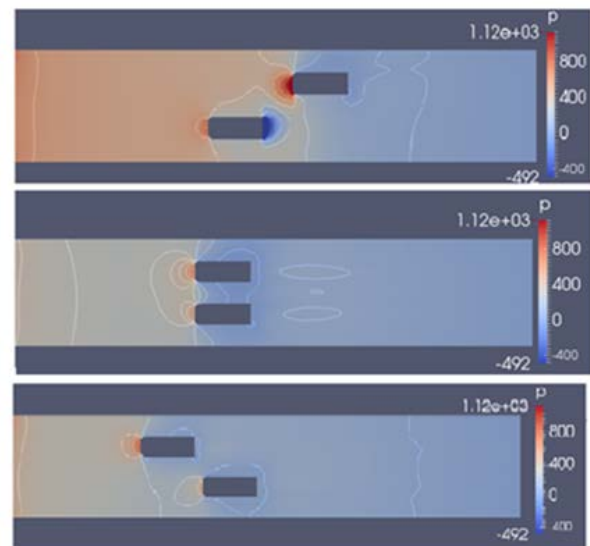


Figure 7a. Pressure contours during the overtaking, top to bottom : yet to overtake, starting to overtake, overtaking accomplished

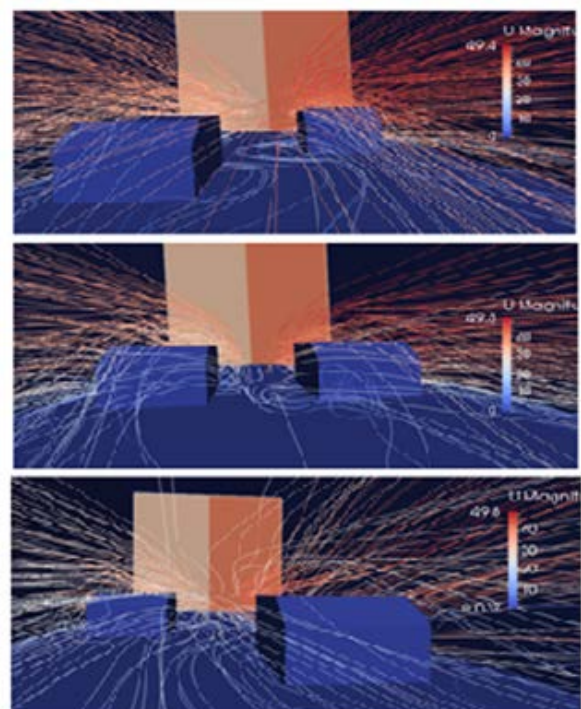


Figure 7b. Stream lines during the overtaking, top to bottom : yet to overtake, starting to overtake, overtaking accomplished

The overtaking vehicle faces a high pressure region at the front as compared to the vehicle to be overtaken. The low pressure exists in the rear end of the overtaking vehicle and vehicle to be overtaken due to the wake region. Intense recirculation of stream lines is clear from the rear view.

Two stations are obtained from each case during overtaking and velocity and turbulent kinetic energy quantities are compared and shown in Figures 8, 9 and 10. Mutual interference of the various separated flow regions, triggered by changes in vehicle speed induces abrupt changes of the overall flow field. Road vehicles move in close proximity to each other and the interaction is common. As observed in Figure 8, the rear point on the slant height (point 'b') is at high velocity on the exterior and shows high intensity in turbulent fluctuations. This is due to the presence of thicker boundary layer growth in the slant surface as opposed to point 'a' that has slightly lower velocity and turbulent kinetic energy. There is a free stream shear layer that merges at a velocity of 38 m/s, while another shear layer created by overtaking vehicle drives the flow at 52 m/s. The drop in turbulent kinetic energy is significant at half the height of the normal distance from the slant height points 'a' and 'b'. The above said trend could also be clearly made for the points 'c' and 'd' on the vehicle to be overtaken, but the intensities are less as found in the overtaking vehicle. This contributes to increase in drag for the overtaking vehicle.

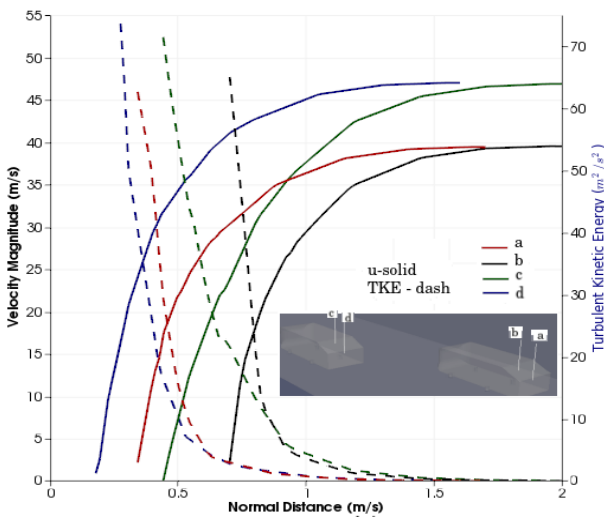


Figure 8. Velocity and turbulent kinetic energy before starting to overtake

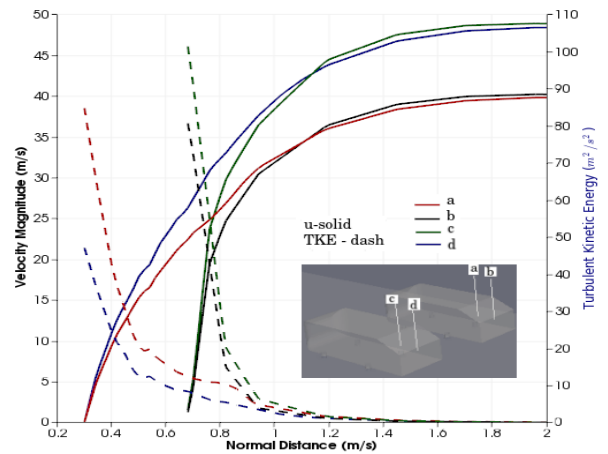


Figure 9. Velocity and turbulent kinetic energy about to overtake

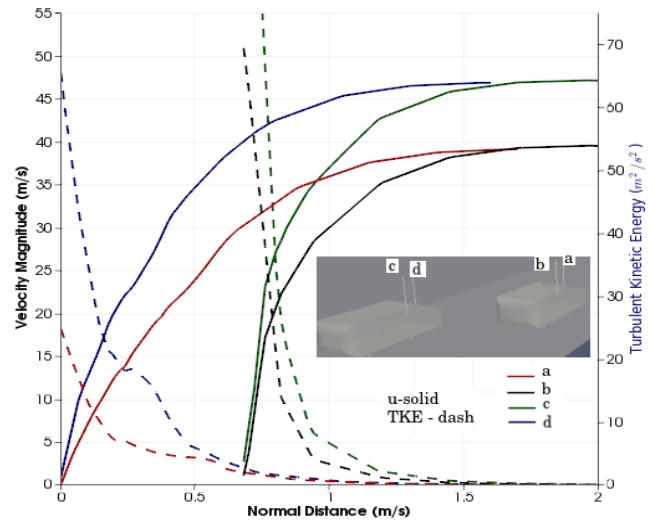


Figure 10. Velocity and turbulent kinetic energy after the overtaking

From the flow field for the overtaking cases, the velocity in boundary layer increases parabolically and found to merge with the other point on the vehicle to be overtaking. This is due to strong interaction between two vehicles at the same location. This improves the flow field and shear layer is reduced as the downstream velocities between two vehicles arise to form an unique and common flowfield at the interface. However, the fluctuations in the flow field indicate the change in turbulent flow field as the disturbance of vehicle is influenced by the other. The points on the rear slant for the overtaken case are mostly similar to the situation of two vehicles side by side. The magnitude of velocity and turbulent kinetic energy merges to the same value for the points 'a-c' and 'b-d'.

**3.4 Platooning**

In the isolated model case, drag and lift coefficients were equal to 0.287 and 0.536, respectively. The concept of vehicle behind another travelling at same speed seems to be of practical interest. The cross-sectional mesh view (Fig. 11) for two cases i.e. inter-vehicle spacing of 0.2 and 0.3 times the vehicle length. However, this case is too complicated in the actual condition on the road. But presently intelligent vehicle for transport can accommodate the inter-vehicular distance of 0.3 times the vehicle distance as the control is purely computerised leading to precise and accurate prediction for braking condition. It has also been observed that vehicle platooning significantly reduces the drag that each vehicle experiences. This reduction of drag translates into less fuel consumption, greater fuel efficiency and less pollution. Drag reduction is found out to be most effective when the distance between vehicles in the platoon is significantly reduced [10].

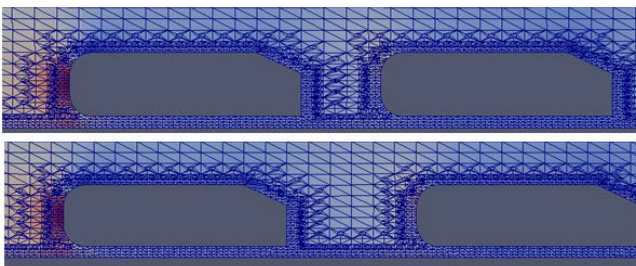


Figure 11. Mesh shown in cross section (side view) for platoon separated by (a) 0.2 times vehicle length (b) 0.3 times the vehicle length

Table 3. Aerodynamic coefficients for platooning case

Gap = 0.2 x vehicle spacing		Gap = 0.3 x vehicle spacing	
C <sub>D</sub>	C <sub>L</sub>	C <sub>D</sub>	C <sub>L</sub>
0.225 (front)	0.519 (front)	0.217 (front)	0.514 (front)
0.313 (back)	0.452 (back)	0.293 (back)	0.462 (back)

Table. 3 shows the lift and drag coefficients for the platooning of two cases as said before. The drag coefficient of the front vehicle is less than that of the rear due to the reduction in wake region for the front vehicle. The drag increases for the rear vehicle as the drag continues to increase along as the inter vehicular spacing is short, as noticed in the case of flow over the flat plate. The

lift of the rear vehicle is significantly less than the front due to the low velocity region at the rear vehicle.

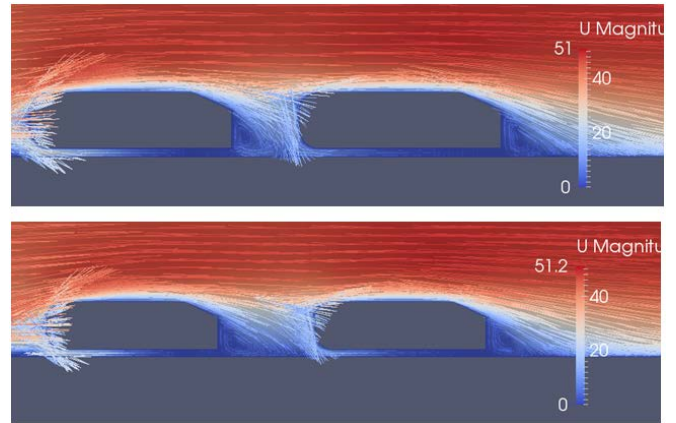


Figure 12. Velocity vectors for platoon separated by (a) 0.2 times vehicle length (b) 0.3 times the vehicle length

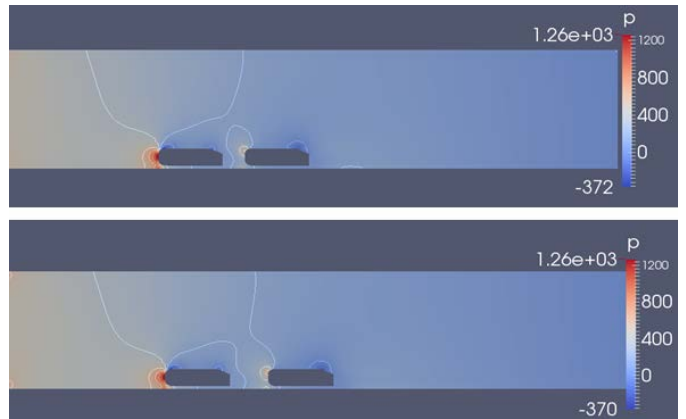


Figure 13. Static pressure contours for platoon separated by (a) 0.2 times vehicle length (b) 0.3 times the vehicle length

The velocity vectors of the two cases of platooning are shown in Fig.12. The flow in the gap between the spacing is similar to lid driven cavity flow but tilted at an angle of 2 degrees at the top wall. The intensity of circulation decreases with the increase in the gap between two vehicles. The static pressure contours are illustrated in Fig. 12. The pressure at the end of the leading Ahmed body is high in the case of higher vehicle spacing. This leads to the effective reduction in drag for case (b). For the lead vehicle, the pressure is higher as it faces the flow whereas the rear vehicle experiences low pressure. It can also be observed that the pressure intermediate to leading and trailing vehicles connects in case (a) well as compared to case (b). It was concluded that the effect of the strong pressure drop arising from the

slant back of the leading vehicle was the cause of the drag and lift changes of the rear vehicle. Since traffic spacing is likely to reduce with the increasing use of intelligent transport systems (ITS), much attention is required in understanding these effects. The effect of the strong vortex system arising from the slant back of the leading vehicle is clearly visible and shown in Fig. 14. The stream lines are much closer to each other in case (a) as compared to case (b). This shows that the higher velocity, thereby leading to lower pressure. The increase in pressure drag is clearly evident in this consideration.

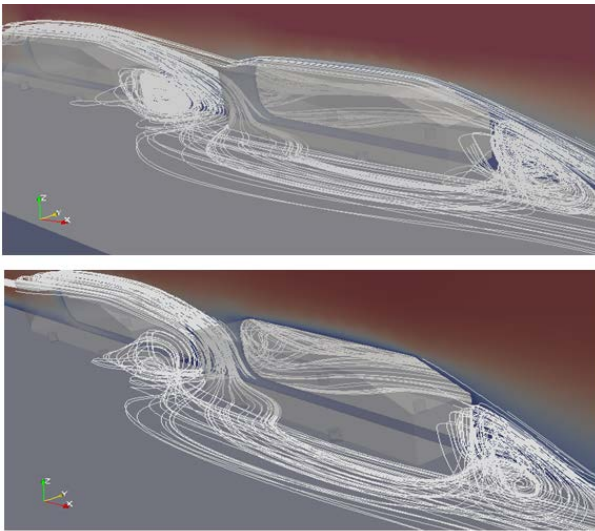


Figure 14. Streamlines comparison top: 0.2 times vehicle length, bottom : 0.3 times the vehicle length

As long as the flow is able to follow the contours of the tail and stays attached the drag reduces. The influence of the incoming flow is investigated, since flow characteristics are changing along the length of the vehicle. The influence of the turbulence kinetic energy on the case (a) leads to a steep rise, whereas the velocity increases to a free stream value at the exterior (Fig. 15). The boundary layer growth behind the vehicles shows fluctuation in the leading vehicle for case (a). Fig. 16 shows the change in the free-stream velocity and sudden change in turbulent kinetic energy at the middle of the normal distance chosen. This contributes to change in the path of flow leading to the drag reduction as compared to case (a).

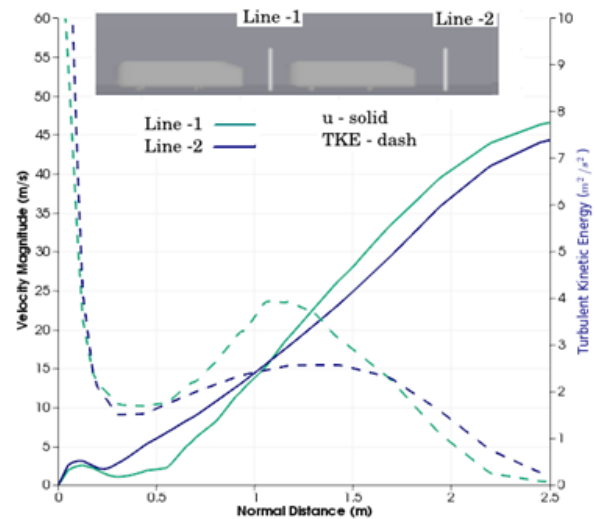


Figure 15. Velocity and turbulent kinetic energy for vehicle separated by 0.2 times vehicle length

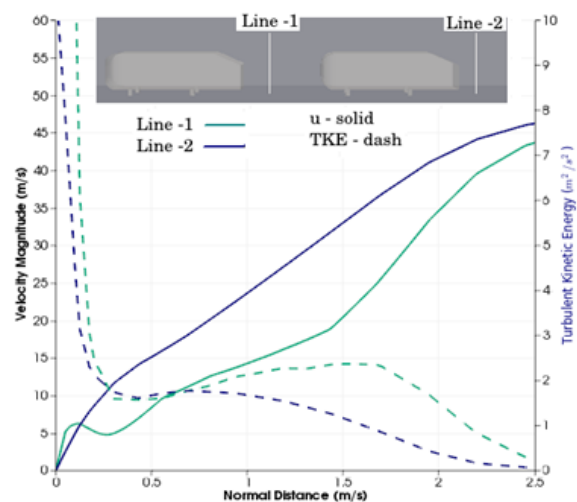


Figure 16. Velocity and turbulent kinetic energy for vehicle separated by 0.2 times vehicle length

## 4. Conclusion

Airflow over the Ahmed body is investigated using the open source software, OpenFOAM to understand the flow processes involved in drag production. The grid independency tests are carried out and compared with the experimental results of Ahmed model. From the study conducted for the acceleration of Ahmed body, it is found that the maximum drag and lift for an Ahmed body vehicle is at higher speeds. Streamlines and pressure contours for the overtaking configurations are studied and compared. The platooning case is numerically investigated to understand the drag reduction for the lead vehicle followed by rear separated by 0.2 and 0.3 times the vehicle lengths. The drag and lift coefficients are significantly reduced for the lead vehicle and rear vehicle respectively.

With the increase in computational power, CFD has become a valuable tool for performing the different cases in vehicle motion simulation and predicting the drag coefficients. Further information on intelligent transport systems in accompanying the drag reduction devices could be the extension from the present work.

*References:*

- [1] Abdel-Azim, A. F., And Abdel Gawad, A. F., 2000, "Numerical Investigation of Vehicles Aerodynamics Through Driving Tunnels," 2000 Future Car Congress, Hyatt Regency Crystal City, Arlington, VA, USA, April 2-6, paper No. 2000-01-1579.
- [2] Abdel Azim, A. F. and Abdel Gawad, A. F., 2000, "A Flow Visualization Study of the Aerodynamic Interference between passenger cars," SAE 2000 world Congress, Detroit, Michigan, USA, March 6-9, paper No. 2000-01-0355.
- [3] Himeno, R., et al., 1990, "Numerical Analysis of the Airflow Around Automobiles Using Multi-block Structured Grids," SAE paper 900319.
- [4] Kitoh, K., et al., 1986, "Effects of Boundary Conditions on Numerical Turbulent Flow Around a Two-Dimensional Vehicle by K- $\epsilon$  model," IIS Annual report of Group, pp. 67-72.
- [5] Ahmed, S. R., and Hucho, W. H., 1977, "The Calculation of the Flow Field Past a Van with the Aid of a panel Method," SAE paper 770390.
- [6] Minato, K., Ryu, H., and Kobayashi, T., 1991, "Aerodynamics of Road Vehicles in Tunnels-Flow Visualization Using the Laser Light Sheet Method and Its Digital Image Processing," Int. Congress and Exposition, Dertroit, MI, USA, SAE
- [7] Ahmed, S.R., Ramm, G., Faltin, G., 1984. Some salient features of the time-averaged ground vehicle wake. SAE Paper 840300.
- [8] OpenFOAM user guide version 2.3.1
- [9] Emmanuel Guilmineau, 2008. Computational study of flow around a simplified car body, Journal of Wind Engineering and Industrial Aerodynamics, Vol. 96 pp. 1207–1217.
- [10] Simon Watkins, Gioacchino Vio (2008), The effect of vehicle spacing on the aerodynamics of a representative car shape, Journal of Wind Engineering and Industrial Aerodynamics, 96 (6–7) pp. 1232-1239.